Autocorrelation Observations with the BIMA Array

Marc Pound and Tamara T. Helfer

ABSTRACT

We report on the current state of autocorrelation capabilities at BIMA. Spectral line observations with window bandwidths <= 50 MHz are reliable, but observations with 100 MHz windows and continuum measurements are not currently feasible. The relative calibration among the individual antennas is typically good to about 20%, and often the agreement among all but one or two of the antennas is better than 10%. The line shapes and strengths of BIMA observations of CO and HCN in IRC+10216 agree to within the noise with spectra from the Bell Labs 7-m and the NRAO 12-m telescopes; a $500'' \times 350''$ BIMA map of $C^{18}O$ from NGC 2024 agrees well in structure with an NRAO 12-m map from the same region, though the emission measured at BIMA is about 20% weaker. Sensitive observations of a weak CS line in MBM12 show that there is no noise floor at the level of at least 16 mK per 24 kHz channel width. The measured rms noise in all the antennas is consistently about 8-15% lower than the theoretical noise; we are unsure of the explanation for this discrepancy. We describe new MIRIAD routines to process autocorrelation spectra and give template observation and data reduction scripts.

1. Introduction

Because of the very good sensitivity of the current BIMA array, it is now practicable to use the interferometer to map extended sources using a mosaic of multiple-pointing observations. It is expected that this will be a routine mode of observing with the Millimeter Array. An important step in making reliable maps of extended emission is filling the central hole in the *uv* plane. At mm wavelengths, this has traditionally been done by measuring the source distribution with a singledish telescope of larger aperture than the interferometer elements. In the "homogeneous array" method, the goal is to achieve a fully-sampled map using the interferometer elements to measure the singledish flux (see e.g., Wilner 1993). With reliable autocorrelation now available, the BIMA array can be used to acquire the zero-spacing data. The advantage of using BIMA for these measurements is the time saved by observing with 9 independent antennas as well as the overhead saved in coordinating observations at two telescopes. Furthermore, telescope-dependent parameters such as gain and beam shape do not complicate the combination of the auto- and cross-correlated data.

2. How An Autocorrelated Spectrum is Measured

With an autocorrelation measurement of an astronomical source S, the dominant signal generally comes from radiation from the sky, with a secondary contribution from the receiver noise; these contaminations must be measured in order to determine the relatively weak signal from the source.

For a receiver with noise temperature T_{Rx}, the power measured in a single channel when looking at an ambient flap at a temperature T_{AMB} is

$$V_{AMB} = \kappa\ (T_{Rx} + T_{AMB}),$$

where κ is the Volts/K conversion.[1] Similarly, the power when looking at blank sky at a temperature T_{SKY} is

$$V_{OFF} = \kappa\ (T_{Rx} + T_{SKY}).$$

The quantity in parentheses is just the system temperature referred to above the atmosphere, so

$$V_{OFF} = \kappa T_{SYS}.$$

When we observe a source at temperature T_S, the signal is

$$V_{ON} = \kappa\ (T_{Rx} + T_{SKY} + T_S).$$

If we solve for T_S and make use of the above relationships, then

$$T_S = \frac{V_{ON} - V_{OFF}}{V_{OFF}} T_{SYS},$$

or

$$T_S = \frac{T_{ON} - T_{OFF}}{T_{OFF}}\ T_{SYS}.$$

In practice, there are i values of these temperatures for i channels in the backend, resulting in arrays of T_S, T_{ON}, T_{OFF}, and T_{SYS}. The final quantity T_S measured by the BIMA antennas is T_A^* as defined by Kutner & Ulich (1981); i.e., it is the source antenna temperature corrected for atmospheric and ohmic losses and rearward spillover. To convert to main beam brightness temperature T_{mb}, one should divide by the main beam efficiency: $T_{mb} = T_A^*/\eta_M$, where η_M is calculated to be 0.83 at 100 GHz for the BIMA antennas and is not a strong function of frequency (Lugten 1994).

---

[1] Note that it is customary to refer to "Volts," even though it is power that is measured; the power is measured by a square-law detector that is linear to first order.

3. Calibration of the Autocorrelation Spectra

From the above expression for the source temperature T_S, we see that the absolute calibration of an autocorrelation spectrum depends on an accurate determination of the system temperatures. The receiver gains and system temperatures are calibrated using the vane (chopper wheel) method (Penzias & Burrus, 1973), where the total powers are measured when the receivers are looking at the blank sky and at a room-temperature load. Since the sky is used as one of the calibration loads, when one measures a signal from an astronomical source (which also travels through the atmosphere), the contribution from the sky cancels out. This calibration scheme works if the ambient load temperature is not too different from that of the sky.

The single sideband receiver gains κ and system temperatures are

$$\kappa = \frac{(V_{amb} - V_{OFF})}{T_{cal}}$$

and

$$T_{sys} = \frac{V_{OFF}}{\kappa},$$

where V_{amb} is the power measured when looking at the ambient load. T_{cal} is the "equivalent calibration temperature" from Ulich & Haas (1976, equation 17); it is the difference between the temperatures of the load and the sky, which is then corrected for the receiver gain, telescope efficiency and atmospheric extinction. T_{cal} is calculated using the outdoor temperature, the airmass, an assumed ambient load temperature, and a frequency-dependent zenith opacity which is calculated using a simple model of the atmosphere. The relative gains of the upper and lower sidebands of the first LO are assumed to be the same. In practice, $T_{cal} \approx 290$ K (DSB) over most of the 3 mm band, though T_{cal} rises steeply with frequency above about 110 GHz because of atmospheric extinction in the wings of the 118.75 GHz O_2 line.

At BIMA, the system temperatures are measured as a function of frequency across the bandpass. Sample channel-by-channel system temperatures, ONs, OFFs, and the resultant T_A^* spectra are shown in Figure 1. Despite the considerable structure across the raw bandpass, the resultant T_A^* spectra usually require only linear baseline[2] removal.

4. Test Results

We made observations of a variety of sources in order to check the consistency of the temperature scales among the individual antennas, to measure the system sensitivity, and to compare BIMA singledish observations with observations from other singledish telescopes.

---

[2]In this document, we use "baseline" in the singledish sense, i.e. "zero signal level," rather than the interferometric usage meaning projected separation of antennas.

4.1. Relative Calibration Among the BIMA Antennas

We observed HL Tau on 1996 Nov 30 in ^{13}CO as a test of a strong ($T_A^* \approx 5$ K), narrow ($\Delta v \approx 1$ km s^{-1} FWHM) line. The spectra, shown in Figure 2, show good baseline stability; linear fits only were removed from the spectra. The pointing accuracy, which is estimated to be $\sim$ 5–10″ rms from interferometric runs, is at most about 10% of the half power primary beamwidth in the 3 mm band; the good relative pointing of the different antennas is reflected in the similarity of the line shapes in Figure 2 as well as those in other sources (e.g. IRC+10216, see Figure 3). The relative calibration among the antennas is reasonably good; the average and standard deviation of the intensity is $< I >= 4.89 \pm 0.86$, a $\pm$ 18% variation. From Figure 2, we see that the calibration of Antenna 6 seems relatively high and that of Antenna 7 relatively low. If we compare the remaining antennas, we find that $< I >_{24589}= 4.86 \pm 0.26$, a $\pm$ 5% variation only. Though the stability of the relative calibration is quite good over the course of a few-hour run, we did see the relative calibration change substantially among our various test observations. In the IRC+10216 CO spectra shown in Figure 3, taken on 1997 Feb 27, Antennas 2, 5 and 7 agree quite well, while Antenna 4 is high by about 11%, Antennas 6 and 8 are low by about 20%, and Antenna 9 is low by 40%. In the MBM12 spectra taken in 1997 Feb 05, the agreement among antennas is better, though Antenna 9 is low by about 10% (Figure 4*b*). In maps of NGC 2024, Antennas 2, 4, 5, and 8 agree to within 5%, but Antennas 7 and 9 are 25–30% lower (Antenna 6 was not used).

4.2. System Sensitivity

To test the sensitivity of the system and to see if there was a noise floor imposed by the correlator, we observed the relatively weak ($T_A^* \approx$ 0.2 K, $\Delta v \approx$ 0.5 km s^{-1} FWHM) CS line from a clump in the high-latitude cloud MBM12 (Figure 4*a*). We found that the rms noise decreases with the square root of time over more than 8 hours of total integration; there is no noise floor at the 16 mK level. The agreement among antennas is better than either the HL Tau or IRC+10216 observations (Figure 4*b*). Furthermore the peak antenna temperature and integrated intensity agree to about 10% with NRAO 12-m data from Pound & Blitz (1993). However, the rms noise in all the antennas is about 12% **lower** than expected from the system temperatures and backend setup (Figure 5). At this time, the reason for this discrepancy is not clear. The effect is independent of antenna number or receiver.

4.3. Comparison With Other Telescopes

In order to check the calibration of the BIMA antennas against that of another telescope, we observed CO from IRC+10216 with BIMA and with the Bell Labs 7-meter telescope. The Bell Labs and BIMA antennas have virtually identical primary beams sizes (BL=96″; BIMA=100″ at 115 GHz) and gains (BL=128 Jy/K; BIMA=120 Jy/K at 115 GHz) and similar main beam

efficiencies (η_M(BL)=0.94, η_M(BIMA)=0.83). Figure 6*a* shows a comparison of the CO spectra from IRC+10216 taken with the two systems. The agreement is excellent–even the small scale features of the line profile are reproduced.

We also compared BIMA observations of HCN in IRC+10216 to published observations (Dayal & Bieging 1995) from the NRAO 12-m telescope. The HCN emission from IRC+10216 is strongest at the center of the source and falls to zero intensity at a diameter of about 64″; the radial profile is roughly gaussian with a FWHM of 21.6″. Since the BIMA FWHM beam width is 132″ and the NRAO 12-m FWHM is 70″ at 89 GHz, this emission is confined to within both beams. The BIMA spectrum is shown in Figure 6*b* along with the NRAO 12-m spectrum from Dayal & Bieging (1995), where the latter has been adjusted to the size of the BIMA beam by multiplying by $(70^2 + 21.6^2)/(132^2 + 21.6^2) = 0.300$. Again, the agreement is excellent.

To test the mapping capabilities, we observed a 500″ × 350″ region of the NGC 2024 molecular ridge in $C^{18}O$ at BIMA and compared it to a map made with the NRAO 12-meter telescope. Figure 7 shows the NRAO map at its full resolution, the NRAO map regridded and smoothed to match the BIMA map, and the BIMA map. The contour shapes and relative intensity of features in the maps agree well, but all features in the smoothed NRAO map are about 20% brighter than in the BIMA map. In the two right panels, we have converted both maps to the main beam brightness temperature scale, using η_M appropriate for each telescope. Because the source is very extended compared to the beam sizes, the use of the main beam efficiency is likely an overcorrection resulting in antenna temperatures that are too high. A correction that takes into account the detailed sidelobe patterns and source brightness distribution may result in closer agreement.

4.4. 100 MHz Bandwidth and Continuum Observations

In any correlator setup that includes 100 MHz windows, there is a time-dependent instability in the baselines, even over the short timescales required for autocorrelation observations ($\lesssim$ 30 sec). An example of this problem is shown in Figure 8. The instability causes a variation in amplitude of several K over the 100 MHz windows, and it appears to vary randomly with time. The cause of this problem is not known, but it may be related to DC bias drifts in the sampler cards (see Hudson 1996). Given this instability, it is not currently feasible to make continuum observations or spectral observations of external galaxies, which generally have line profiles that are both very broad and very weak. For smaller-bandwidth observations, the baseline curvature is typically linear or quadratic over the passband, and it may removed by polynomial fitting to the emission-free region of the spectra.

5. Data Acquisition and Reduction

5.1. Integration Time

In order to combine autocorrelation and crosscorrelation maps effectively, the scaled noise levels must be comparable; if anything, one wants the autocorrelation map to have somewhat lower noise. The required rms for the autocorrelation map depends on how one plans to combine it with the interferometric map. For large mosaics it may be most convenient to work in the image plane with the MIRIAD task MOSAIC. In this case, one should match the rms noise in the autocorrelation map with that of the crosscorrelation map with which it is to be combined, and the needed autocorrelation rms is the determined by ratio of the primary to synthesized beam areas:

$$\sigma_T^{auto} = \left(\frac{\Omega_{pb}}{\Omega_{syn}} \right) \sigma_T^{cross}.$$

The total (ON+OFF) integration time t_{auto} necessary to reach a desired sensitivity can be estimated using the radiometer equation,

$$\sigma_T^{auto} = \frac{2\ T_{SYS}}{\eta_{corr}\sqrt{N \Delta\nu\ t_{auto}}}, \tag{1}$$

where N is the number of antennas, $\Delta\nu$ is the frequency resolution in Hz, and $\eta_{corr} = 0.87$ is the efficiency of a 2-bit correlator. Note that the frequency resolution is **not** equal to the channel spacing because the correlator windowing function is a `sinc` in the frequency domain, which causes an effective broadening by a factor of 1.21. The factor of 2 in the numerator assumes that one spends an equal amount of time ON and OFF the source: one factor of $\sqrt{2}$ is because only half of the integration time t_{auto} is spent looking on the source, and another $\sqrt{2}$ comes from taking the difference between ON and OFF measurements. Note that this efficiency can be pushed higher if the sky is stable. For Hanning smoothed spectra (see § 5.2), where the frequency resolution is degraded by another factor of 1.65, equation 1 becomes

$$\sigma_T^{auto} = \frac{1.63\ T_{SYS}}{\sqrt{N \Delta f\ t_{auto}}}, \tag{2}$$

where Δf is now the channel spacing. The autocorrelation integration time t_{auto} is then

$$t_{auto} = \left(\frac{1.63\ T_{SYS}}{\sigma_T^{auto}} \right)^2 (\Delta f\ N)^{-1}. \tag{3}$$

Alternatively, if one does the combination in the *uv* plane instead of in the image plane, one would want to match the sensitivity in the central hole filled in by the singledish data to that of the *uv* tracks immediately surrounding it. In this case, a good rule of thumb is to plan to spend the same total time on-source in autocorrelation mode as in crosscorrelation mode, so that

$$t_{auto} = \frac{2}{N} t_{cross},$$

where t_{cross} is the total on-source integration time in the crosscorrelation map. Whether one does the combination in the image plane or in the *uv* plane, one should ensure that the sensitivity of singledish data is not the limiting factor.

5.2. Sample Observing Script

Autocorrelation observations are currently carried out using the task XMINT at Hat Creek. XMINT is the same as the usual observing program MINT with the exception that the T_{SYS} spectra are saved and written out as standard MIRIAD visibilities. To distinguish the T_{SYS} spectra from source data, the T_{SYS} spectra are held in the arrays that are usually used for polarization data and are tagged as `pol(XX)`.

Below we provide a sample observing script which makes a 3×3 map of OrionA in ^{13}CO and C^{18}O. The spectra are taken one row at a time, interleaving OFFs with ONs. Note that the OFF **must** be first in order for the MIRIAD autocorrelation reduction task SINBAD to work properly (§ 5.3). The ONs and OFFs are specified by the `grid` parameter `ON(...)`, with OFFs taking the value 0 and ONs taking the value 1. The number of arguments passed to `ON(...)` must equal the number of grid points. In this example, the grid scale is set to 0.875 for Nyquist sampling of the 105″ primary beam. One could observe multiple ONs per OFF if the sky is stable enough. Generally, Antennas 1 and 3 are not used for autocorrelation, since they slew much more slowly than the rest of the array. The MIRIAD routine XCORF may be used with the `auto` checkbox selected to define the correlator setup. It is a good idea to use `coptions=auto,nocable,hanning` to turn off cable length measurements explicitly and to Hanning smooth the data. Without Hanning smoothing, strong sidelobes of the `sinc` windowing function can appear in the spectrum. Hanning smoothing reduces the sidelobe level from 0.22 to 0.027 while degrading the frequency resolution by 1.65 (see, e.g., Rohlfs 1987; Thompson, Moran, & Swenson 1986).

When using BIMA in autocorrelation mode, all the usual caveats for singledish observing apply, e.g. the need for clean and nearby OFF positions, integration times appropriate for sky conditions, and frequent enough calibration. Also note that autocorrelation mode is inherently double sideband – since there is no phase information, the sidebands of the first LO are not separated and lines from both sidebands will appear in the same window. This also means that continuum observations, once they are feasible, will yield fluxes that are too high by a factor of two and will need to be corrected by hand accordingly.

```
#!/bin/csh -f
#
# Autocorrelation observing template script
#
```

```
# use only fast-slewing antennas.
set ants=2456789

# Setups
setup name=all nchan=1 maxobs=2 itime=30 nreps=1,2 lstrange=0145,0925 \
elevlim=20 ants=$ants task=xmint

set name=tune freq=109.78216 iffreq=300 $ants\
        dopcat=$UCAT/you.cat obsline=co dopsrc=OrionA

setup name=corsetup cormode=4 coptions=auto,nocable,hanning $ants\
        corf=312.5,275,731,690 corbw=25,50,25,50 \
        restfqs=109.78216,109.78216,110.201353,110.201353

setup name=row1 setup=all source=OrionA catalog=$UCAT/you.cat \
        vis=orion ants=$ants stop=+20  scale=0.875\
        grid="DRA(60,-1,60,0,60,1),DDEC(0,0,0,0,0,0),ON(0,1,0,1,0,1)"

setup name=row2 setup=all source=OrionA catalog=$UCAT/you.cat \
        vis=orion ants=$ants stop=+20 scale=0.875\
        grid="DRA(60,-1,60,0,60,1),DDEC(1,1,1,1,1,1,1),ON(0,1,0,1,0,1)"

setup name=row3 setup=all source=OrionA catalog=you.cat \
        vis=orion ants=$ants stop=+20 scale=0.875\
        grid="DRA(60,-1,60,0,60,1),DDEC(-1,-1,-1,-1,-1,-1),ON(0,1,0,1,0,1)"

# Observing
scan setup='tune'
scan setup='corsetup'
loop srcsetup='row1,row2,row3'
```

5.3. Data Reduction

When XMINT is run with `coptions=auto`, the arrays of ON and OFF are written as channel amplitudes (T_A^* times `jyperka`^{2}) in the MIRIAD visibility format, with all channel phases set to zero, 180, or –180. The arrays are distinguished by the *uv* header variable `on`, and can be isolated in MIRIAD tasks with the standard `select` keyword. The system temperature scans are written as usual visibilities whenever a calibration is done; the T_{SYS} scans are distinguished by the label `pol(XX)` (see Table 1). Although the T_{SYS} arrays are stored in polarization arrays, there is no real polarization information contained in the scans.

The standard MIRIAD reduction path for autocorrelation data is SINBAD → SINPOLY → VARMAP → IMCOMB. The task SINBAD takes the autocorrelation "visibility" file and calculates $T_A^* = T_{SYS}$ (ON–OFF)/OFF, writing the result to the user-specified output file. Polynomial baselines may then be removed from the T_A^* spectra using the task SINPOLY. VARMAP is used to make one MIRIAD image for each antenna from the baselined data, and IMCOMB averages the images. Inspection of data and flagging of bad channels are accomplished in the usual way with UVSPEC and UVFLAG. The only difference is that one should look at the real values not the amplitudes.

Table 1: Summary of MIRIAD autocorrelation format

SCAN	**on** value	pol	type	select
ON	0	YY	real	on
OFF	1	YY	real	-on,pol(yy)
TSYS	−1	XX	real	-on,pol(xx)

```
#/bin/csh -f
#
# Template autocorrelation data reduction script
#
# inspect the data
uvspec vis=orion nxy=3,3 axis=chan,real device=/xw

# make Tsys*(ON-OFF)/OFF
sinbad vis=orion out=orion.sinbad

# remove 2nd-order baselines from each window, averaging over 5 minutes
sinpoly vis=orion out=orion.sinpoly interval=5 device=/xs nxy=3,3 \
   options=window npoly=2,2,2,2 badchan=4,200,300,600,700,1000,1100,1400,1500

# make maps of the first window for each antenna
foreach ant ( 2 4 5 6 7 8 9 )
   varmap vis=orion.sinpoly cell=53,53 imsize=3,3 \
          select=ant'('$ant'),window(1)' out=map.$ant
end

# Combine the images with no weighting.
# If you wish the images to have specific weights, you must compute
# them accordingly
imcomb in='map.*.scaled' out=map.avg rms=1,1,1,1,1,1,1
```

6. Unsolved Problems and Suggestions

1. There are time-dependent instabilities in the broad-bandwidth measurements that preclude continuum and extragalactic spectral line observations (§ 4.4).

2. The antenna temperature scales are different from antenna to antenna, and the difference is a function of time (§ 4.1).

3. The measured rms noise is lower than the theoretical noise by 8-15% on all antennas (§ 4.2).

4. Continuum observations, if they were feasible, would have fluxes that are a factor of 2 too high (§ 5.2). We suggest putting a flag on the continuum setup in SETCORR in order to get the flux right.

5. The current observing method of one grid list per map row is klutzy, especially if one wants to make a large map. As the map grows the list of `setup name=rowN` grows, as does the `grid=` list. Some standard map grids should be decided upon and corresponding grid files which include the OFF positions and the ON(...) list should be made. The map ONs and OFFs could be integers between, say, –10 and 10, and the user would set the scale appropriate to the observing frequency (primary beam size).

6. Some FITS i/o is needed for individual scans. A small modification to the MIRIAD routine FITS to write out spectral scans would be adequate.

7. The `select` interface should be changed so that `select=on(-1)` chooses T_{SYS} scans, `select=on(0)` chooses OFFs, and `select=on(1)` chooses ONs. Currently one specifies `on` or `-on` and `pol` to get the desired type.

8. There is no quality assessment for autocorrelation. The Hat Creek task "quality" is not meant for autocorrelation data. Some quality control would be nice.

9. It would be useful for SINBAD to allow averaging of OFFs. This would allow observing with balanced OFF positions. Also SINBAD doesn't add up the integration time correctly.

We thank Wilson Hoffman, Jerry Hudson, Lynn Urry, Jack Welch, and Mel Wright, who are responsible for most of the hardware and software used for these measurements. We thank Bob Wilson and Greg Wright for providing spectra from the Bell Labs telescope, and John Bieging for providing the NRAO 12-m HCN spectrum of IRC+10216.

REFERENCES

Dayal, A. and Bieging, J.H. 1995, ApJ, 439, 996

Hudson, J.A. 1996, BIMA memo #46.

Kutner, M.L. & Ulich, B.L. 1981, ApJ, 250, 341

Lugten, J.B. 1994, Proc. of the European Workshop on Low-Noise Quasi-Optics, ed. N. J. Keen, J. Lamb, and G. A. Ediss

Penzias, A.A. & Burrus, C.A. 1973, ARA&A, 00, 00.

Pound & Blitz 1993, ApJ, 418, 328

Rohlfs, K., 1987, *Tools of Radio Astronomy*, 156ff.

Thompson, A., Moran, J., & Swenson, G. 1986, *Interferometry and Synthesis in Radio Astronomy*, 236ff.

Ulich, B.L. & Haas, R.W. 1976, ApJS, 30, 247

Wilner, D. 1993, BIMA memo #35.

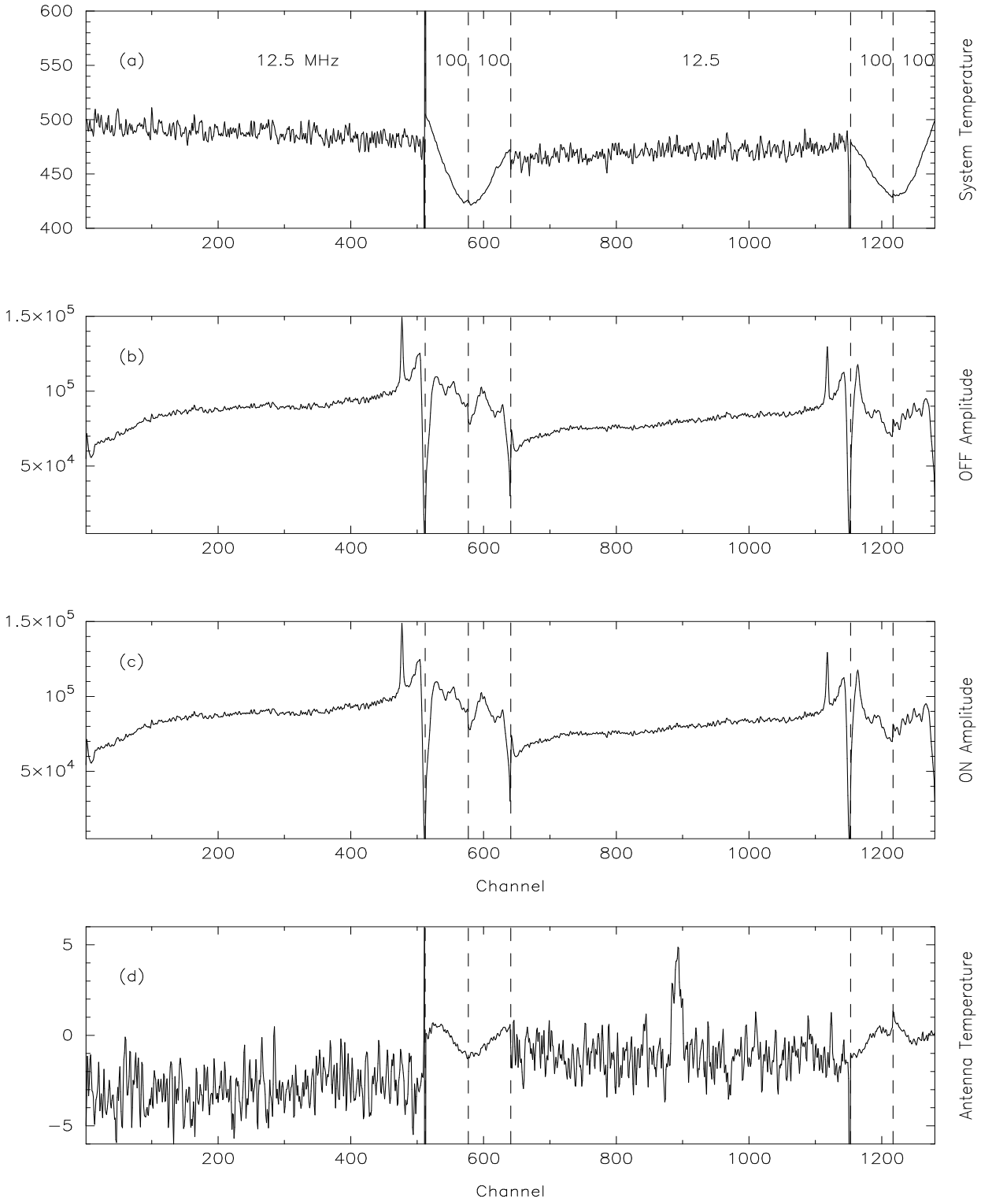

Fig. 1.— Example raw and processed spectra from a mode 6 observation. Individual windows are indicated by the dotted lines. (*a*) Typical T_{SYS} scan. (*b*) Typical OFF scan. (*c*) Typical ON scan. (*d*) T_A^* spectrum resulting from a, b, and c.

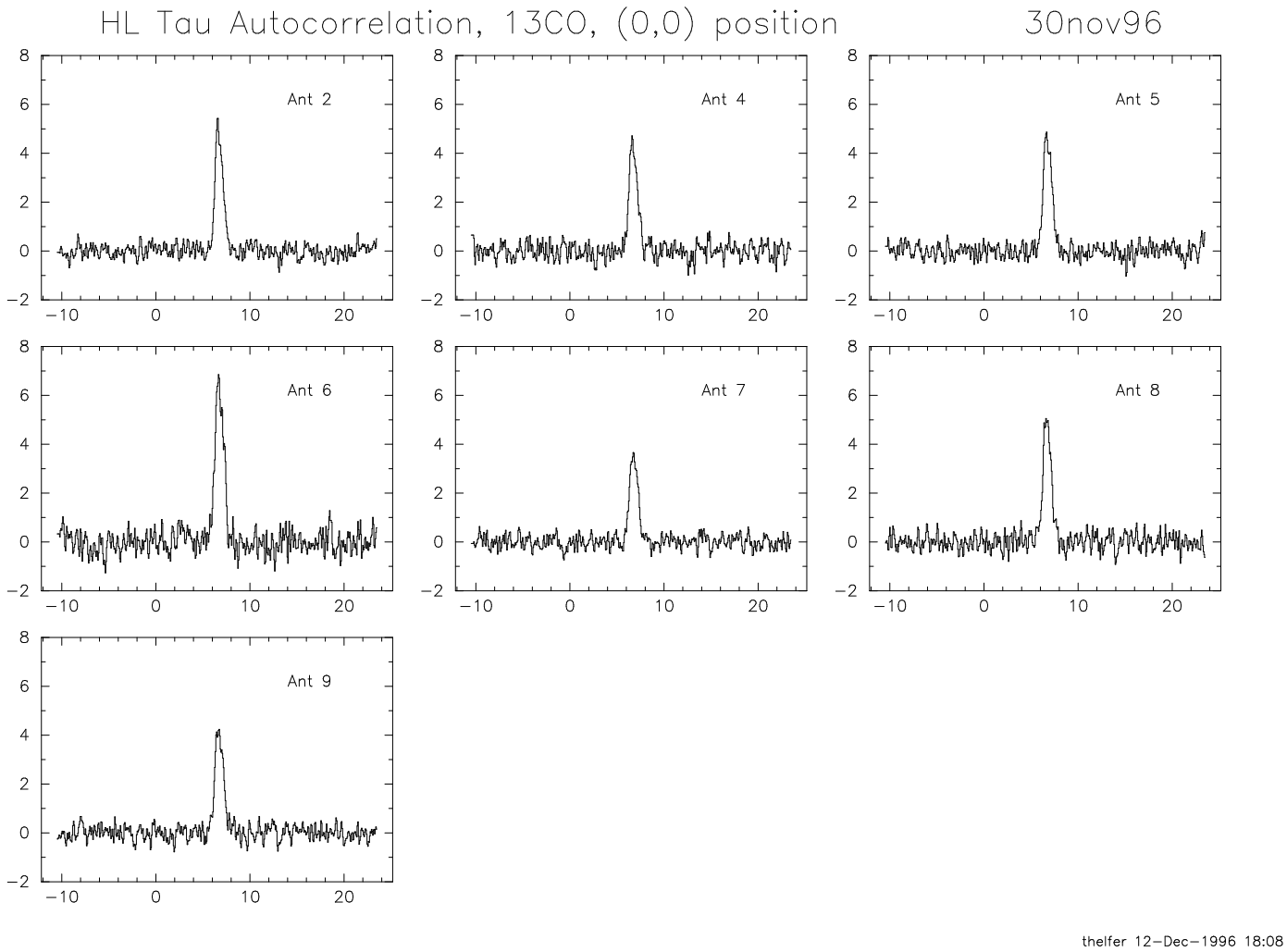

Fig. 2.— ^{13}CO spectra from individual antennas of a strong source, HL Tau, taken 30 Nov 1996. Shown are the 12.5 MHz windows from mode 6. Linear baselines were fit and removed using the emission-free regions of the spectra.

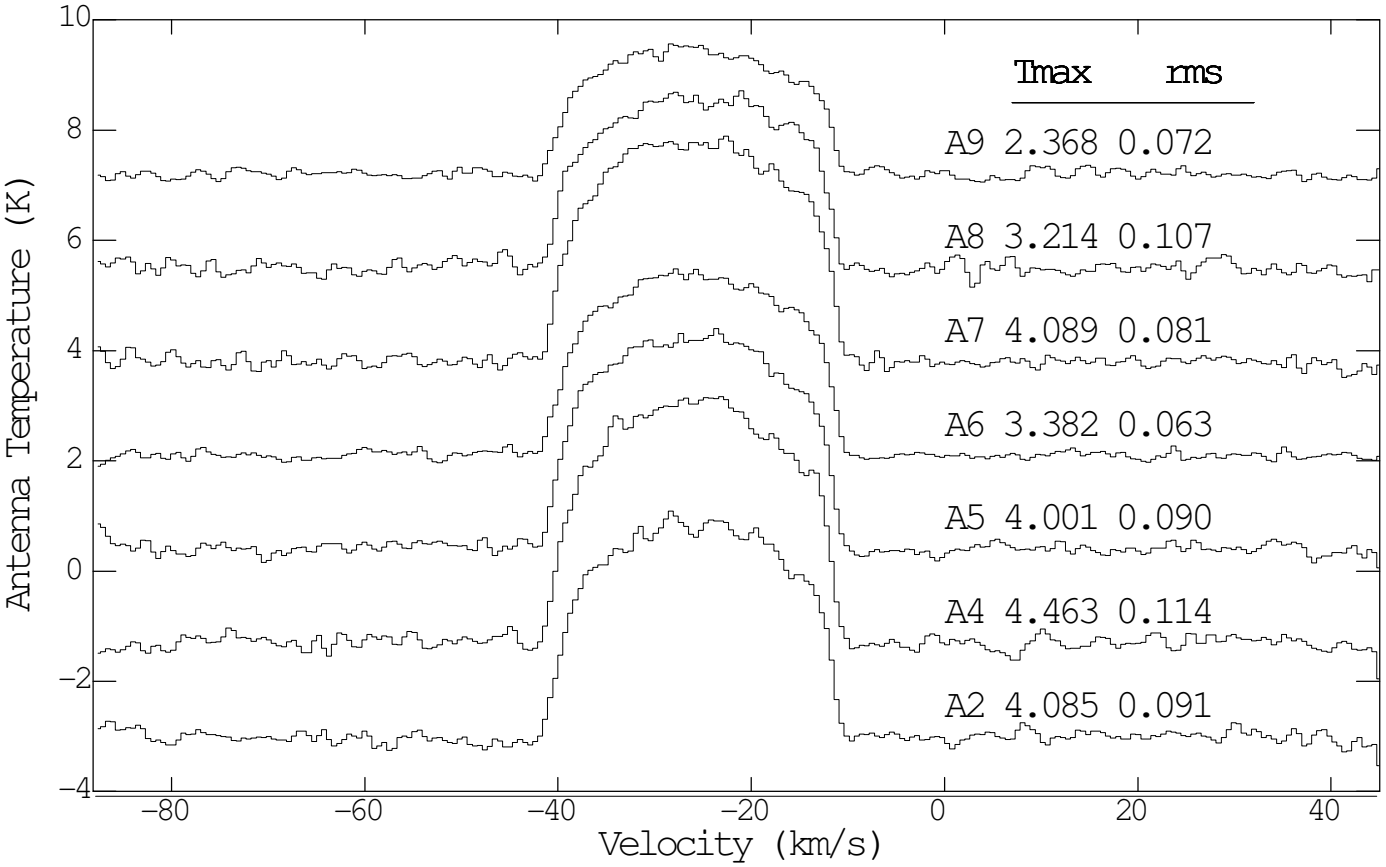

Fig. 3.— ^{12}CO spectra of IRC+10216 from individual antennas taken in mode 4 on 27 Feb 1997. The spectra are 25 MHz windows with 0.2 MHz channel spacing. Second order baselines were removed from all the spectra except for that of Antenna 8 which needed a 4th order fit. The numbers on the right of the plot give the peak temperature and rms of each spectrum.

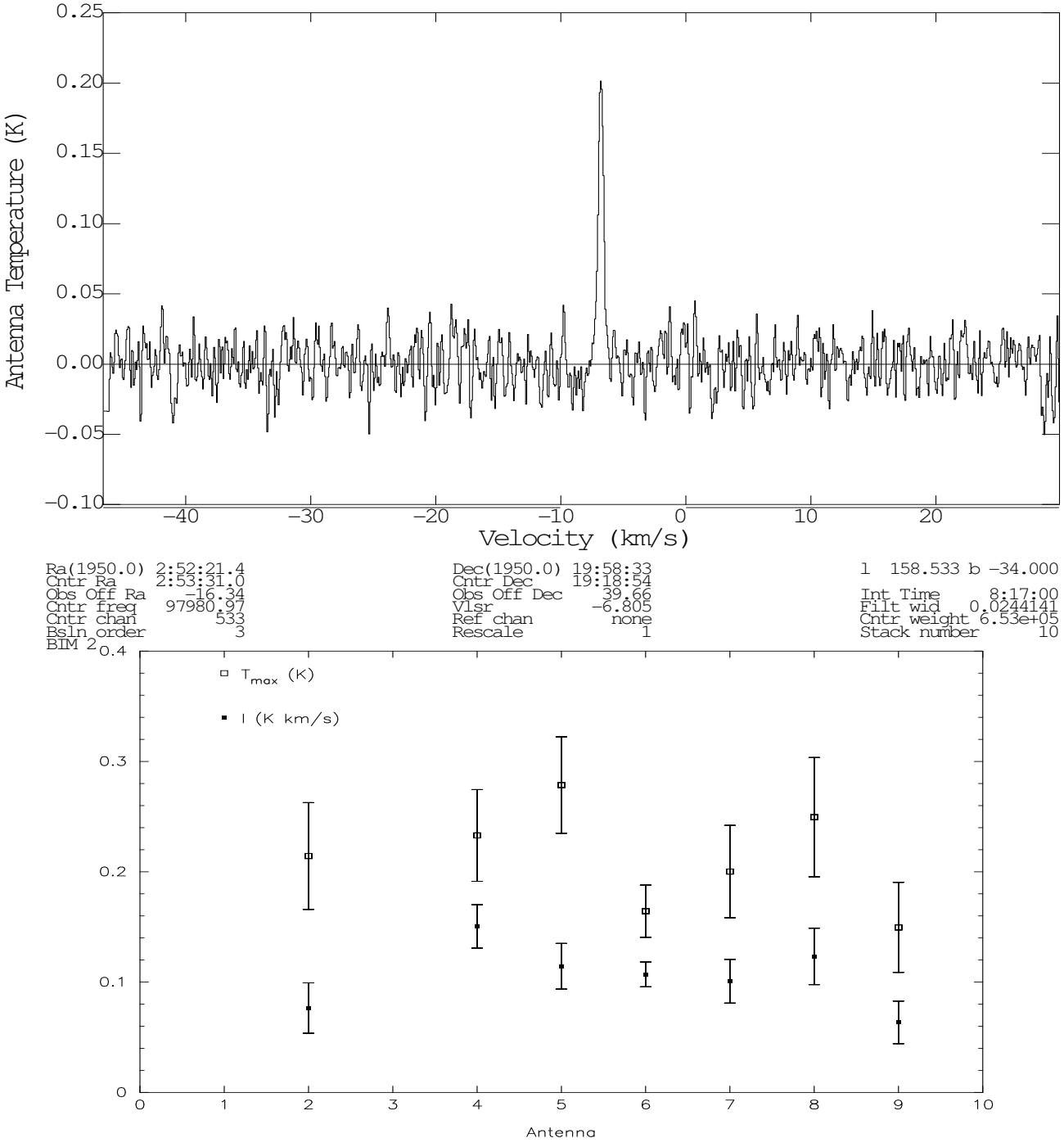

Fig. 4.— (*upper*) Co-added spectrum of a weak source, MBM12-1 in L1457, taken on 05 Feb 1997. This combination of all antennas gives a total integration time of 8h 17m (7 antennas times 71 minutes). The rms is 0.016 K. The spectrum has a 3rd order baseline removed to get rid of a low-level ripple with amplitude ~ 0.005 K. (*lower*) Inter-antenna comparisons of peak temperature and integrated intensity for MBM12-1 for the 71 minute co-added spectra. The error bars are 1 σ. The agreement between antennas is very good. At the time of the observations, antenna 6 was equipped with a new Engargiola receiver and had system temperature about half of the other antennas.

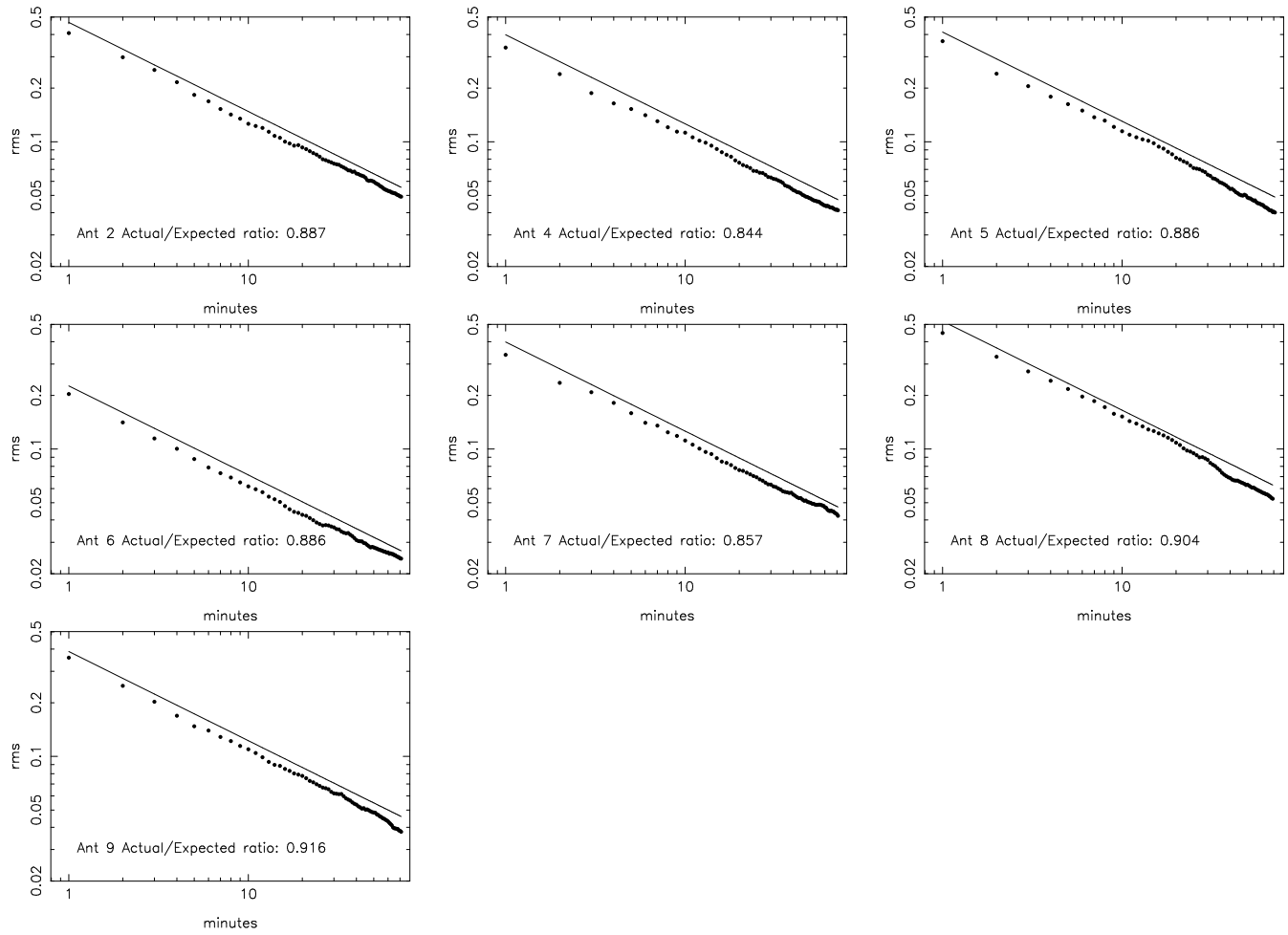

Fig. 5.— Actual and expected rms noise over the 71 minutes of MBM12-1 observations. The solid line is the theoretical rms predicted from equation 2 using the average system temperature for each antenna. The system temperatures varied by less than 5% over the 71 minute interval. The symbols show the actual rms, which is 8-15% lower than expected on all antennas.

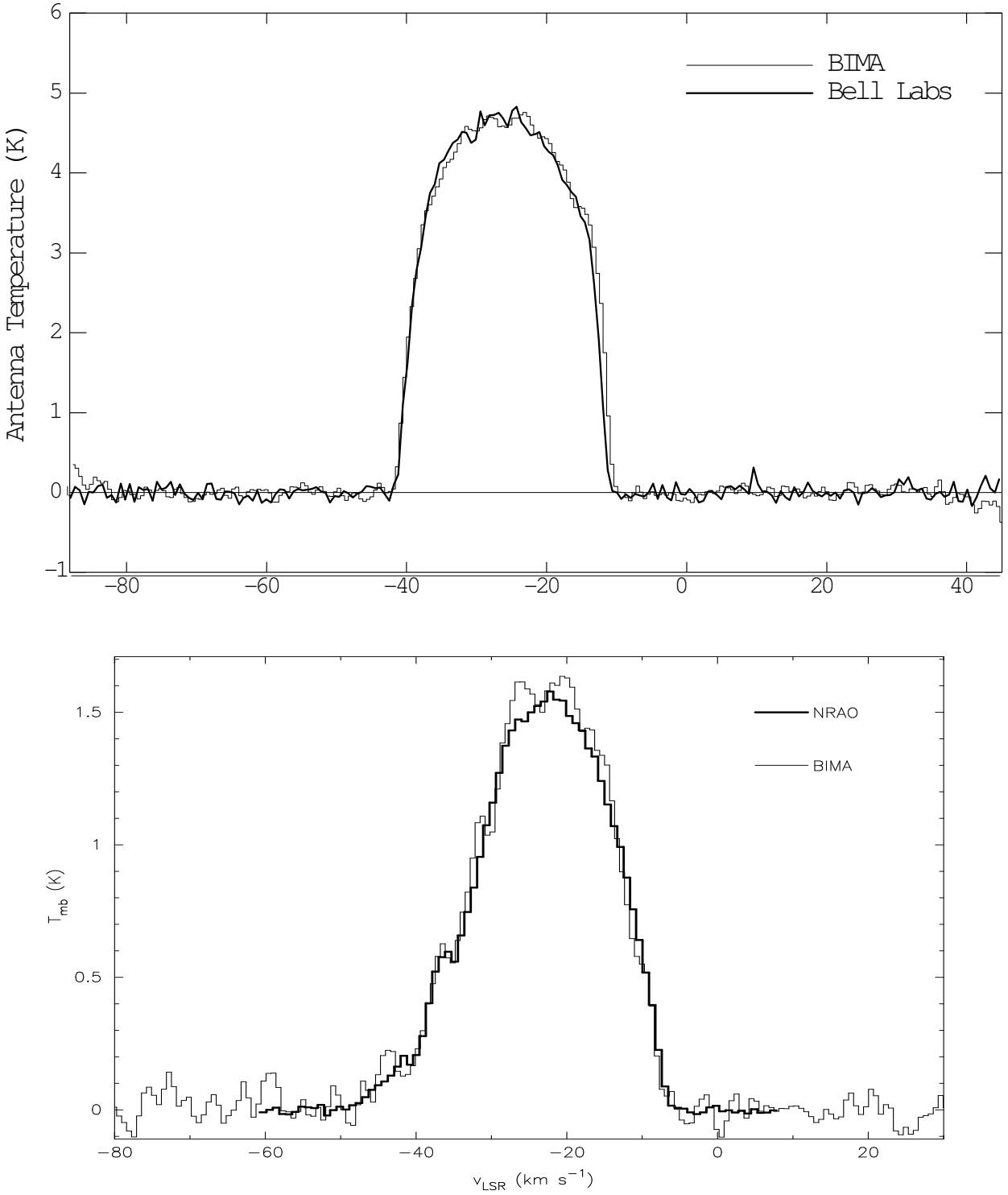

Fig. 6.— (*upper*) ^{12}CO spectra of IRC+10216, on main beam brightness scale. Thin line: co-add of BIMA antennas 2, 5 and 7. Heavy line: Spectrum from Bell Labs 7-meter telescope. (*lower*) HCN spectra of IRC+10216. Thin line: co-add of BIMA antennas 2, 4, 5, 6 and 7. Heavy line: NRAO 12-m spectrum, convolved to the size of the BIMA beam (see § 4.3).

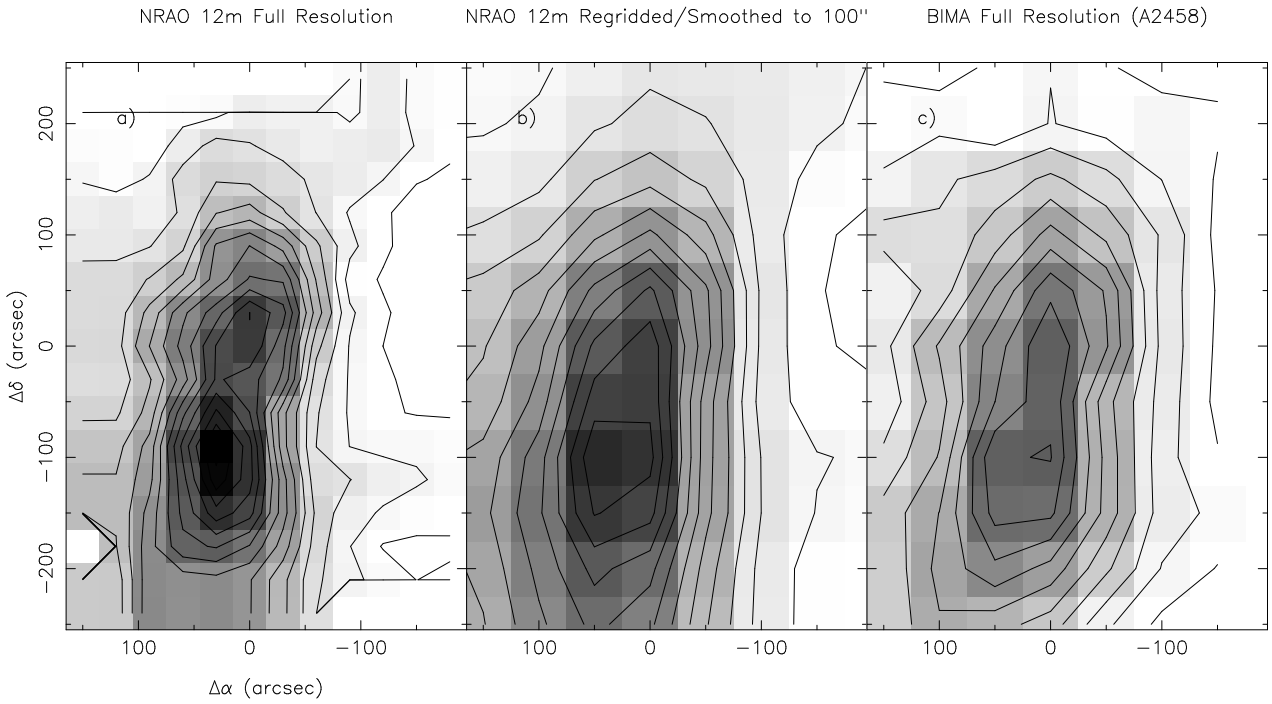

Fig. 7.— a) $C^{18}O$(1-0) integrated intensity map of NGC 2024 made with the NRAO 12-meter; b) same map smoothed to the BIMA resolution; c) Averaged BIMA map from Antennas 2,4,5, and 8 Contours are 0.8 K km/s intervals starting at 0.8 K km/s and grayscale is 1.2 to 12 K km/s for all three maps. Maps (b) and (c) are on main beam brightness temperature scales and may be directly compared. Map (a) is on T_R^* scale.

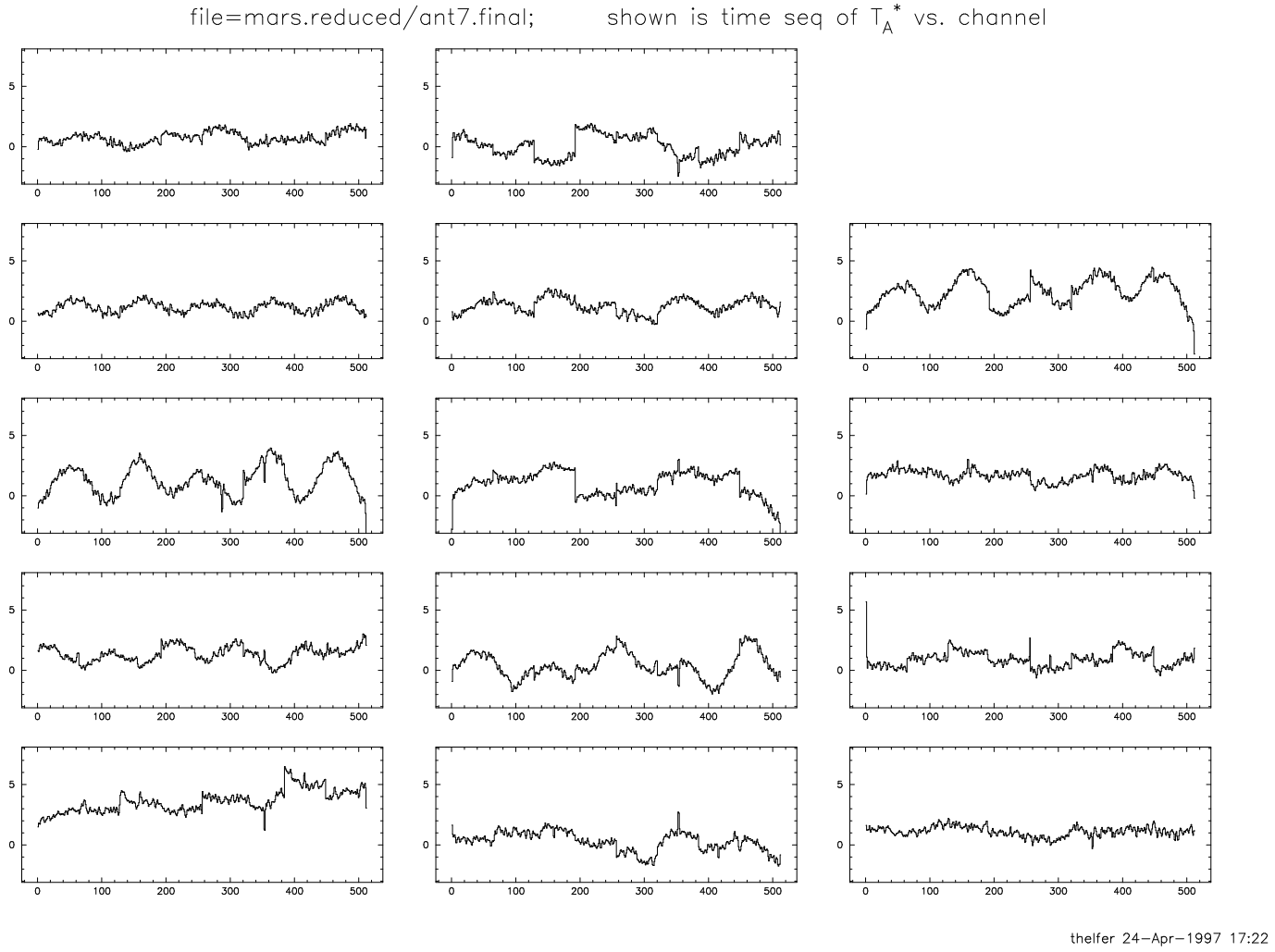

Fig. 8.— An example of the baseline ripple in mode 8. Shown is a time sequence of T_A^* spectra from antenna 7; each spectrum results from a 15-second ON and a 15-second OFF pair. The time sequence starts at the lower left panel. The 100 MHz window edges are apparent every 64 channels as breakpoints in the spectra.